THE JOURNAL OF BIOLOGICAL CHEMISTRY VOL. 285, NO. 23, pp. 17471–17478, June 4, 2010
Printed in the U.S.A.

Incorporation of Tyrosine and Glutamine Residues into the Soluble Guanylate Cyclase Heme Distal Pocket Alters NO and O_2 Binding*[S]

Received for publication, December 22, 2009, and in revised form, March 13, 2010 Published, JBC Papers in Press, March 15, 2010, DOI 10.1074/jbc.M109.098269

Emily R. Derbyshire[‡1], **Sarah Deng**[§], **and Michael A. Marletta**[‡¶‖2]

From the Departments of [‡]*Molecular and Cell Biology,* [§]*Plant and Microbial Biology, and* [¶]*Chemistry and the* [‖]*Division of Physical Biosciences, Lawrence Berkeley National Laboratory, University of California, Berkeley, California 94720*

Nitric oxide (NO) is the physiologically relevant activator of the mammalian hemoprotein soluble guanylate cyclase (sGC). The heme cofactor of $\alpha1\beta1$ sGC has a high affinity for NO but has never been observed to form a complex with oxygen. Introduction of a key tyrosine residue in the sGC heme binding domain $\beta1$(1–385) is sufficient to produce an oxygen-binding protein, but this mutation in the full-length enzyme did not alter oxygen affinity. To evaluate ligand binding specificity in full-length sGC we mutated several conserved distal heme pocket residues ($\beta1$ Val-5, Phe-74, Ile-145, and Ile-149) to introduce a hydrogen bond donor in proximity to the heme ligand. We found that the NO coordination state, NO dissociation, and enzyme activation were significantly affected by the presence of a tyrosine in the distal heme pocket; however, the stability of the reduced porphyrin and the proteins affinity for oxygen were unaltered. Recently, an atypical sGC from *Drosophila*, Gyc-88E, was shown to form a stable complex with oxygen. Sequence analysis of this protein identified two residues in the predicted heme pocket (tyrosine and glutamine) that may function to stabilize oxygen binding in the atypical cyclase. The introduction of these residues into the rat $\beta1$ distal heme pocket (Ile-145 → Tyr and Ile-149 → Gln) resulted in an sGC construct that oxidized via an intermediate with an absorbance maximum at 417 nm. This absorbance maximum is consistent with globin Fe^{II}-O_2 complexes and is likely the first observation of a Fe^{II}-O_2 complex in the full-length $\alpha1\beta1$ protein. Additionally, these data suggest that atypical sGCs stabilize O_2 binding by a hydrogen bonding network involving tyrosine and glutamine.

Soluble guanylate cyclase (sGC)[3] is the most thoroughly characterized receptor for the gaseous signaling agent nitric oxide (NO). NO induced activation of sGC is critical to several physiological processes, including neurotransmission, vasodilation, and platelet aggregation (1–3). The importance of sGC to physiological function has been clearly demonstrated over the last decade (4, 5); however, much less is understood about the molecular mechanisms that regulate enzyme activity.

sGC is a heterodimeric hemoprotein consisting of two homologous subunits, α and β. The $\alpha1\beta1$ heterodimer is the most prevalent and commonly studied protein. Despite the same histidine ligated heme and iron oxidation state as found in the globins, sGC shows no measurable affinity for O_2 and therefore can selectively bind NO in the presence of O_2 (reviewed in Refs. 6, 7). Interestingly, not only does sGC discriminate against O_2 binding to the heme, but both the Fe^{II}-unligated and Fe^{II}-NO species are stable in an aerobic environment (8). This is in stark contrast to other hemoproteins that readily bind and ultimately react with O_2 (9–12). The mechanism by which sGC discriminates against O_2 binding as well as the molecular events that lead to activation remain to be elucidated.

There have been several proposals on the mechanism of ligand discrimination in sGC (7, 13, 14) and most recently a model was developed based on the crystal structure of a sGC heme domain homologue from *Thermoanaerobacter tengcongensis* (*Tt*) (see Fig. 1) (15, 16). This protein is part of the heme-nitric oxide and oxygen (H-NOX) binding family, the members of which all share sequence homology with the heme domain (residues 1–190 of the rat $\beta1$ subunit) of sGC. The crystal structure revealed that *Tt* H-NOX stabilizes O_2 binding via a hydrogen bonding network primarily involving a tyrosine and a tryptophan (Tyr-145 and Trp-9 as defined by the rat numbering system, see alignment (Fig. 1)). An asparagine residue (Asn74) is also involved in this hydrogen bonding network, but site-directed mutagenesis has shown that Asn-74 is less critical than Tyr-145 and Trp-9 for O_2 stabilization (13). Based on multiple sequence alignments, $\alpha1\beta1$ sGC lacks these hydrogen bonding residues, and therefore it was proposed that the lack of these amino acids contributes to the ability of sGC to discriminate against O_2 binding (13). This proposal was called into question in recent reports that showed that the introduction of a tyrosine in the $\beta1$ subunit at a position that aligns with *Tt* H-NOX Tyr-145 in full-length sGC does not yield an O_2-binding protein (17, 18) despite the fact that this point mutant in the sGC heme-binding construct $\beta1$(1–385) was able to bind O_2 (13).

To further evaluate O_2 binding in sGC we examined several predicted sGCs by multiple sequence alignments and homol-

* This work was supported, in whole or in part, by National Institutes of Health Grant GM077365 (to M. A. M.).

[S] The on-line version of this article (available at http://www.jbc.org) contains supplemental Figs. S1–S4 and Table S1.

[1] Present address: Harvard Medical School, Dept. of Biological Chemistry and Molecular Pharmacology, Boston, MA 02115-5701.

[2] To whom correspondence should be addressed: University of California, Berkeley, Dept. of Chemistry, 570 Stanley Hall, Berkeley, CA 94720-1460. Tel.: 510-666-2763; Fax: 510-666-2765; E-mail: marletta@berkeley.edu.

[3] The abbreviations used are: sGC, soluble guanylate cyclase; NO, nitric oxide; H-NOX, heme-nitric oxide and oxygen binding domain; YC-1, 3-(5′-hydroxymethyl-3′-furyl)-1-benzylindazole; DEA/NO, diethylammonium (*Z*)-1-(*N*,*N*-diethylamino)diazen-1-ium-1,2-diolate; DTT, dithiothreitol; Sf9, *Spodoptera frugiperda*; *RZ*, ratio of apo- to heme-bound protein; *Tt*, *Thermoanaerobacter tengcongensis*.

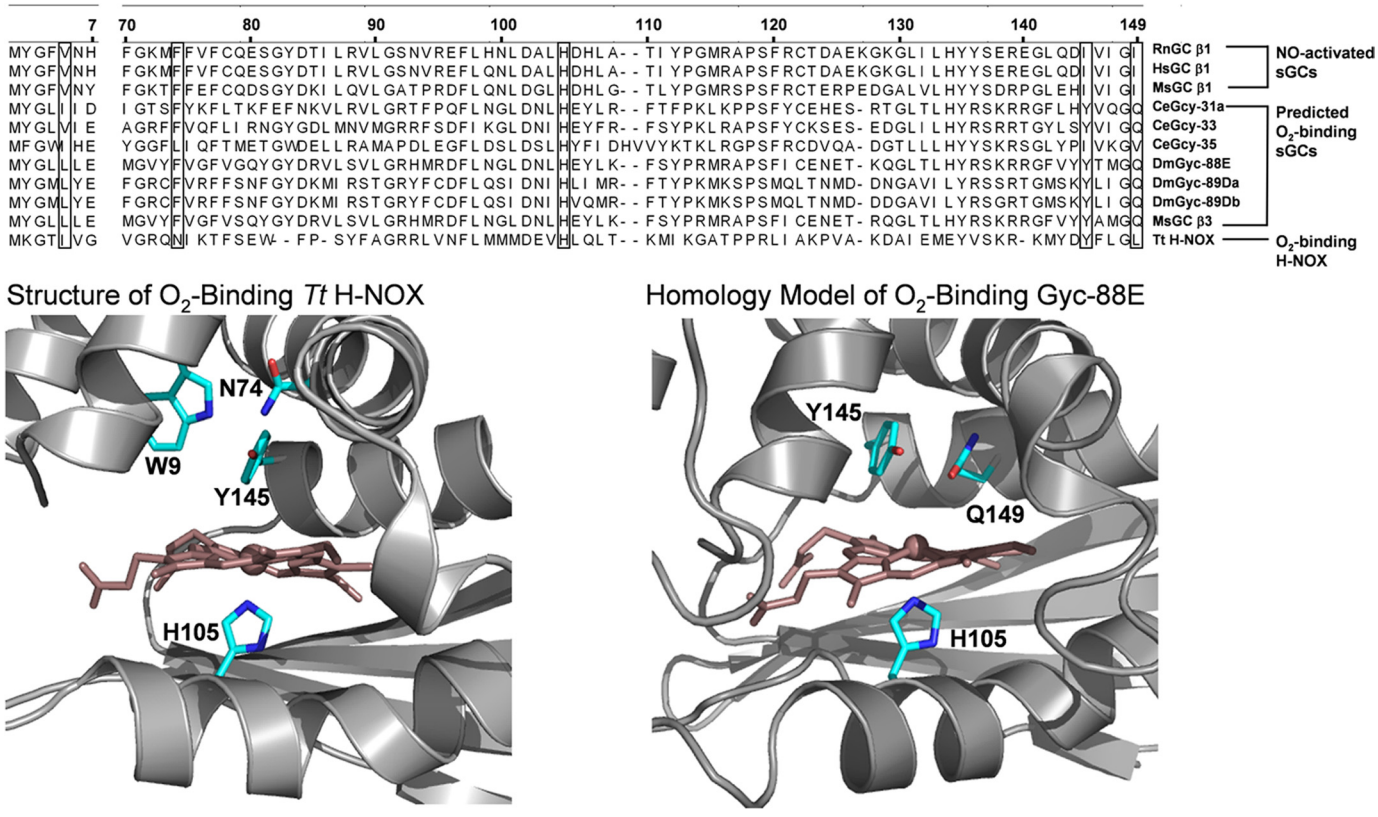

FIGURE 1. **Alignment of NO-activated sGCs with predicted O_2-binding sGCs.** Numbering is that of the rat β1 protein. Structure of *Tt* H-NOX (*left*) and homology model of O_2-binding Gyc-88E H-NOX domain (*right*) are shown. The *Tt* H-NOX structure shows that O_2 is stabilized at the heme by a hydrogen bonding network involving Trp-9, Asn-74, and Tyr-145 (1U55.pdb) (*W9, N74*, and *Y140* in the *Tt* H-NOX numbering system). The homology model of the O_2-binding Gyc-88E suggests that residues capable of stabilizing O_2 binding, including Tyr-145 and Gln-149, are in the distal heme pocket (Y143 and Q147 in the Gyc-88E numbering system).

ogy modeling (Fig. 1). Several sGCs that do contain a tyrosine that aligns with the *Tt* H-NOX Tyr-145 are found in organisms ranging from insects like *Drosophila melanogaster* (19) to vertebrate fish such as *Oncorhynchus mykiss*. Based on the presence of this tyrosine it is predicted that these sGCs have the potential to bind O_2, and indeed one such protein, Gyc-88E from *D. melanogaster*, has been isolated and shown to bind O_2 (20). Like some GAF domain-containing proteins (DevS (21) and DosT (22)), and known globin-coupled sensors (23–25), this O_2-binding guanylate cyclase likely requires this tyrosine for O_2 ligation. Although these atypical O_2-binding sGCs, like Gyc-88E, lack the tryptophan and asparagine known to be important for O_2 binding in *Tt* H-NOX, multiple sequence alignments suggest another possible hydrogen bond donor is present in the heme distal pocket: glutamine. A homology model of Gyc-88E suggests that this glutamine is in proximity to both the distal pocket tyrosine and O_2 bound to the heme. Additionally, this residue is conserved in sGCs that contain a tyrosine in the predicted heme distal pocket.

Based on the presence of both a tyrosine and a glutamine in the predicted heme distal pocket of Gyc-88E, and the precedence of tyrosine/glutamine hydrogen bonding networks in other heme-binding proteins (26–28), we propose that O_2-binding sGCs utilize these amino acids to stabilize O_2 binding, and, therefore, the absence of these residues is critical for the ability of $\alpha1\beta1$ sGC to discriminate against O_2. Significantly, we found that the reactivity of $\alpha1\beta1$ sGC with O_2 was altered with the introduction of the proposed Gyc-88E hydrogen bonding network (tyrosine/glutamine), but not the *Tt* H-NOX hydrogen bonding network (tyrosine/tryptophan). These data support the hypothesis that the lack of a hydrogen bonding network in the sGC distal heme pocket is critical to the mechanism of ligand discrimination in non O_2-binding sGCs. Additionally, this report evaluates sGC activation after mutagenesis of conserved heme pocket residues that are proposed to play an important role in maintaining the proteins heme conformation (16).

EXPERIMENTAL PROCEDURES

Materials—Primers were obtained from Elim Biopharmaceuticals. Sf9 cells were obtained from the Dept. of Molecular and Cell Biology Tissue Culture Facility, University of California, Berkeley. Rat sGC $\alpha1\beta1$ was purified as described previously (29). 3-(5′-Hydroxymethyl-3′-furyl)-1-benzylindazole (YC-1) and the NO donor diethylammonium (*Z*)-1-(*N*,*N*-diethylamino)diazen-1-ium-1,2-diolate (DEA/NO) were purchased from Cayman Chemical Co. CO gas was from Praxair.

Site-directed Mutagenesis—Mutants of full-length rat $\beta1$ were generated using the QuikChange XL site-directed mutagenesis kit (Stratagene) according to the manufacturer's instructions. The accuracy of each substitution was verified by sequencing (University of California, Berkeley DNA Sequencing Facility). The Bac-to-Bac baculovirus expression system (Invitrogen) was used to generate recombinant baculovirus

according to the manufacturer's protocol. Sf9 cells were cultured, and recombinant sGC mutants were purified according to a previously published protocol (29). The protein purity of all sGC mutants was assessed by SDS-PAGE using pre-cast 10% Tris-glycine gels (Invitrogen) and was routinely greater than 95%. Protein concentrations were determined using the Bradford Microassay (Bio-Rad Laboratories).

Purification of sGC α1β1 I145Y/I149Q—The sGC purification was slightly modified for sGC α1β1 I145Y/I149Q due to the instability of the construct under standard purification conditions. The cell pellet from 5 liters of Sf9 expression cultures was lysed, and the supernatant was applied to nickel-nitrilotriacetic acid Superflow resin (Qiagen) as described previously. The fractions containing sGC were pooled and exchanged into buffer A (25 mM triethanolamine, pH 7.4, 150 mM NaCl, 5 mM DTT, 10% glycerol) before loading onto a prepacked POROS HQ2 anion-exchange column (Applied Biosystems). A gradient was developed from 150 mM to 500 mM NaCl, and purified sGC was collected and pooled.

Heme Reconstitution—sGC α1β1 F74Y and I145Y/I149Q were isolated with a sub-stoichiometric amount of heme. To reconstitute these proteins 1.5 equivalents of hemin was added to the protein and the sample was left on ice for 12 h to allow the solution to equilibrate. Excess hemin was then removed by applying the sample to a PD-10 column equilibrated with buffer A for sGC α1β1 I145Y/I149Q or buffer B (50 mM Hepes, pH 7.4, 50 mM NaCl, 5 mM DTT) for sGC α1β1 F74Y. Heme stoichiometry was determined as described previously (30). These proteins were characterized both as isolated and after heme reconstitution to ensure the procedure did not affect protein activity or ligand binding characteristics.

Electronic Absorption Spectroscopy—Absorption spectra were collected on a Cary 3E spectrophotometer with a Neslab RTE-100 temperature controller set at 20 °C. Spectra were collected over the range of 250–700 nm at 600 nm/min with a 1 nm data point interval. Reduced (ferrous, Fe^{II}) sGC and the Fe^{II}-CO and Fe^{II}-NO complexes were examined. As purified, most constructs were in the Fe^{II}-unligated state. If the protein as isolated was oxidized (ferric, Fe^{III}), it was reduced by adding 1 mM dithionite in an anaerobic chamber (Coy), and then excess dithionite was removed by three cycles of dilution/concentration using a 10K Ultrafree-0.5 centrifugal filter device (Millipore) into 50 mM Hepes, pH 7.4, 50 mM NaCl. The sGC Fe^{II}-CO complex was formed by flushing CO(g) over sGC in the Fe^{II}-unligated state in a sealed anaerobic cuvette. The Fe^{II}-NO complex was formed by adding 100 μM DEA/NO to Fe^{II}-sGC. After forming the Fe^{II}-NO complex, the effect of temperature on the coordination state was examined. In these experiments the temperature was varied between 5 and 50 °C in the presence and absence of the substrate GTP (1 mM) or the allosteric sGC activator YC-1 (150 μM) in 50 mM Hepes, pH 7.4, 50 mM NaCl, 3 mM $MgCl_2$.

Activity Assays—Duplicate end-point assays were performed at 37 °C as previously described (31). A 10 mM DEA/NO solution was prepared in 10 mM NaOH and a 15 mM YC-1 solution was prepared in DMSO. NO (100 μM DEA/NO) or CO(g) was added to sGC (233 nM) in 50 mM Hepes, pH 7.4, 50 mM NaCl in an anaerobic cuvette. After complex formation was confirmed by electronic absorption spectroscopy the protein was added to an assay mixture to initiate the enzyme reaction. The final assay contained 0.2 μg of enzyme in 50 mM Hepes, pH 7.4, 1 mM DTT, 3 mM $MgCl_2$, 1.5 mM GTP, and 150 μM YC-1 where indicated. All assays were in a final volume of 100 μl and had a concentration of 2% DMSO, which was shown not to affect enzyme activity. Reactions were quenched after 3 min by the addition of 400 μl of 125 mM $Zn(CH_3CO_2)_2$ and 500 μl of 125 mM Na_2CO_3. cGMP quantification was carried out using a cGMP enzyme immunoassay kit, Format B (Biomol), per the manufacturer's instructions. Each experiment was repeated 2–4 times to ensure reproducibility.

Dissociation of NO from sGC—Dissociation of NO from the heme of sGC was measured at 25 °C using the CO/dithionite trapping method described previously (29). The final concentration of $Na_2S_2O_4$ in the reaction mixture was 30 mM, and the final sGC concentration was 1.3 μM. The reaction was monitored by electronic absorption spectroscopy using a Cary 3E spectrophotometer equipped with a Neslab RTE-100 temperature controller. Data were collected over the range of 380–450 nm at 909 nm/min with a 1.5 nm data point interval. Spectra were recorded every 18 s for 5 min, every 1 min for 10 min, and every 2 min thereafter for a total of 3 h, or until the reaction was complete. A buffer baseline was subtracted from each spectrum, and spectra were corrected for baseline drift by normalization to an isosbestic point at ~410 nm. Values for the change in absorbance at 424 nm were extracted from the difference spectra and plotted *versus* time to obtain dissociation time courses for each experiment. Data were fit to single and double exponential equations.

$$\Delta A_t = \Delta A_T(1 - e^{-k_1 t}) \quad \text{(Eq. 1)}$$

$$\Delta A_t = \Delta A_1(1 - e^{-k_1 t}) + \Delta A_2(1 - e^{-k_2 t}) \quad \text{(Eq. 2)}$$

Determination of Autooxidation Rates—The stability of Fe^{II} α1β1 I145Y/I149Q in the presence of O_2 was examined with electronic absorption spectroscopy. sGC was reduced as described above and buffer-exchanged into 25 mM triethanolamine, pH 7.4, 150 mM NaCl, 5 mM DTT, 10% glycerol. Protein (600 nM in 75 μl) in an anaerobic cuvette was monitored over time after the addition of 20 μl of O_2-saturated buffer at 10 °C. The change in the absorbance maximum *versus* time was plotted, and the data were fit to a single exponential (Equation 1).

RESULTS AND DISCUSSION

Introduction of a Single Distal Pocket Tyrosine—The inability of sGC α1β1 to bind O_2 enables the protein to function as a selective NO sensor. Despite predictions based on H-NOX proteins, the reactivity of the α1β1 heterodimer toward O_2 was not affected by mutation of β1 isoleucine 145 to tyrosine (17). To further investigate the mechanism of ligand discrimination in sGC several sGC mutants were examined to test the importance of a single tyrosine and a hydrogen bonding network in the heme distal pocket. To first probe the effects of a single distal pocket tyrosine on the ligand-binding properties of full-length sGC, the β1 mutants V5Y, F74Y, I145Y, and I149Y were purified as heterodimers and characterized. Like the wild-type protein, all of these constructs were isolated in the Fe^{II}-unli-

TABLE 1

Electronic absorption peak positions for various $\alpha1\beta1$ sGC heme pocket mutants at 20 °C

Numbering is that of the rat protein.

Mutation	sGC state	Coordination state	Soret	α/β[a]	*RZ*[b]
			nm	*nm*	
wt	Fe^{II}	5	431	562	0.91-0.67
	Fe^{II}-NO	5	399	572/537	
	Fe^{II}-CO	6	423	567/541	
$\beta1$ V5Y	Fe^{II}	5	433	563	0.53
	Fe^{II}-NO	5	399	573/546	
	Fe^{II}-CO	6	423	570/546	
$\beta1$ F74Y	Fe^{II}	5	428	559	0.15-0.13
	Fe^{II}-NO	5/6	399/416	574/538	
	Fe^{II}-CO	6	423	572/539	
$\beta1$ I145Y	Fe^{II}	5	429	561	0.57
	Fe^{II}-NO	6/5	416/399	574/543	
	Fe^{II}-CO	6	423	568/534	
$\beta1$ I149Y	Fe^{II}	5	431	559	0.57
	Fe^{II}-NO	5	398	570/536	
	Fe^{II}-CO	6	420	568/546	
$\beta1$ L9W/I145Y	Fe^{II}	5	431	558	0.33
	Fe^{II}-NO	5/6	400/416	575/544	
	Fe^{II}-CO	6	423	573/533	
$\beta1$ I145Y/I149Q	Fe^{II}	5	426	556/530	0.09
	Fe^{II}-NO	5/6	399/416	566/533	
	Fe^{II}-CO	6	420	565/536	

[a] These bands were estimated based on positions in two to three spectra collected with 800 nM protein. The low amounts of protein prevent a more absolute assignment.
[b] *RZ*, the ratio of the Soret peak absorbance of the Fe^{II} protein to that at 280 nm.

gated state, and they did not oxidize in air or form a complex with O_2. The ratio of apo- to heme-bound protein (*RZ* value) was estimated from the ratio of the absorbance of the reduced protein at ~431 nm to 280 nm and was used as a measure of heme affinity (Table 1). Assuming the changes in the extinction coefficients of the mutants are small, the ratio of apo- to heme-bound protein can be compared among the constructs to evaluate relative heme affinity. Most of the single distal pocket tyrosine mutants had *RZ* values that were slightly lower than the wild-type protein (Table 1). However, $\alpha1\beta1$ F74Y had a very low *RZ* value (*RZ* ~ 0.15) indicating the protein was isolated with significantly less heme. The mutant was reconstituted with heme to yield a protein that bound ~1 equivalent of heme (*RZ* = 0.70). $\alpha1\beta1$ F74Y exhibited similar ligand-binding properties pre- and post-reconstitution and was enzymatically active (see below), which suggests that the procedure did not disrupt the heme binding pocket. As shown in Fig. 2, the mutants formed stable complexes with both NO and CO. Generally, 6-coordinate CO complexes were characterized by Soret absorbance maxima at 420 or 423 nm, but significant variability was observed in the α/β bands (Table 1). This indicates that the α and β bands of sGC Fe^{II}-CO complexes are sensitive to substitutions made within the distal heme pocket.

Interestingly, the electronic absorption maxima for the Fe^{II}-NO complexes showed significant variation (Table 1). Both $\alpha1\beta1$ V5Y and $\alpha1\beta1$ I149Y formed a 5-coordinate NO complex, like the wild-type protein, while $\alpha1\beta1$ F74Y and $\alpha1\beta1$ I145Y formed a mixture of a 5- and 6-coordinate NO complexes.

The sGC homologues *L2* H-NOX and *Tt* H-NOX bind NO as a mixture of 5- and 6-coordinate complexes. Extensive characterization of these proteins revealed that the equilibrium between the 5- and 6-coordinate states could be thermally shifted (32); increasing temperature led to the breaking of the Fe-His bond thus increasing the population of 5-coordinate Fe^{II}-NO. The temperature dependence of the NO coordination state in both $\alpha1\beta1$ F74Y and $\alpha1\beta1$ I145Y (Fig. 3 and supplemental Fig. S1) was examined. In agreement with results obtained with *L2* H-NOX and *Tt* H-NOX, the population of 5-coordinate Fe^{II}-NO increased in a temperature-dependent manner. This thermal equilibrium provided a new method to test the proposal that both substrate (GTP) and a sGC activator (YC-1) weaken the sGC Fe-His bond (33, 34) by examining the temperature

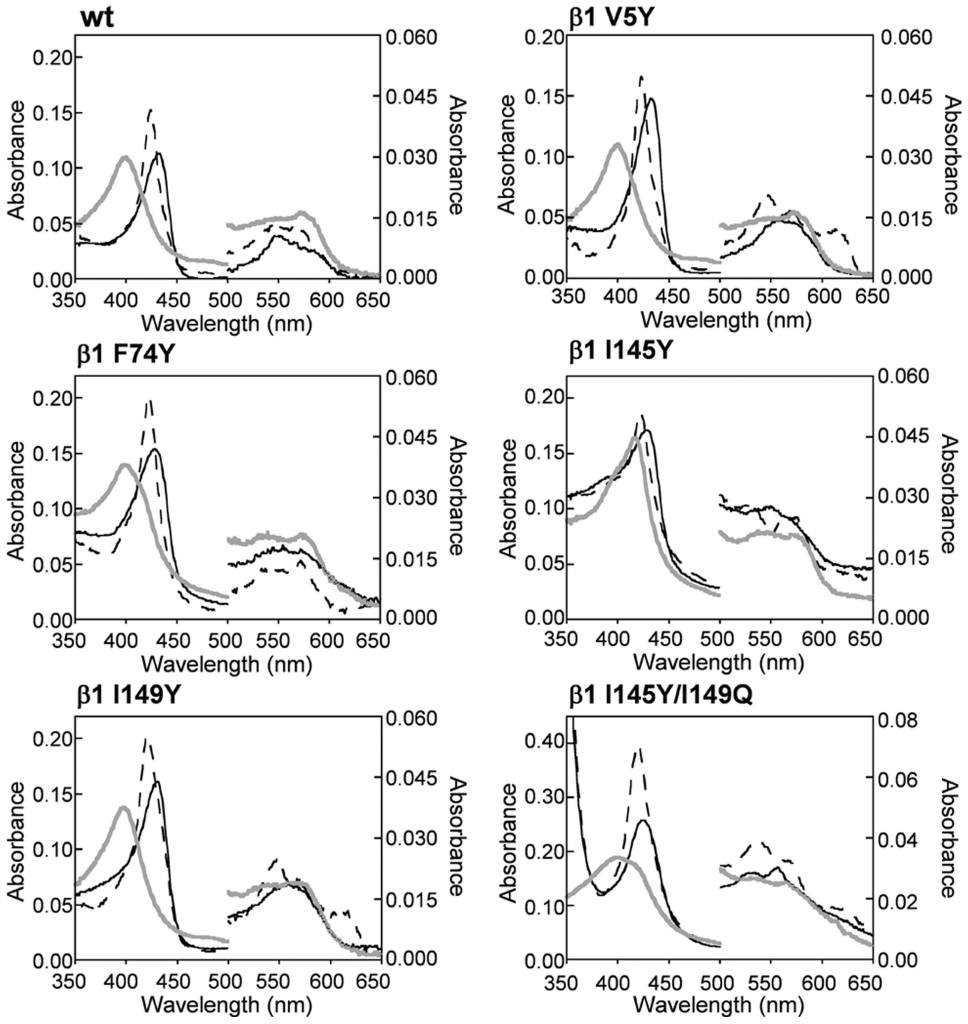

FIGURE 2. **Electronic absorption spectra of sGC $\beta1$ distal pocket mutants at 20 °C.** sGC Fe^{II}-unligated (*black solid line*), Fe^{II}-CO (*black dashed line*), and Fe^{II}-NO (*gray solid line*) complexes are shown for wild-type $\alpha1\beta1$, $\alpha1\beta1$ V5Y, $\alpha1\beta1$ F74Y, $\alpha1\beta1$ I145Y, $\alpha1\beta1$ I149Y, and $\alpha1\beta1$ I145Y/I149Q. All single point mutants do not bind O_2 or oxidize after exposure to air.

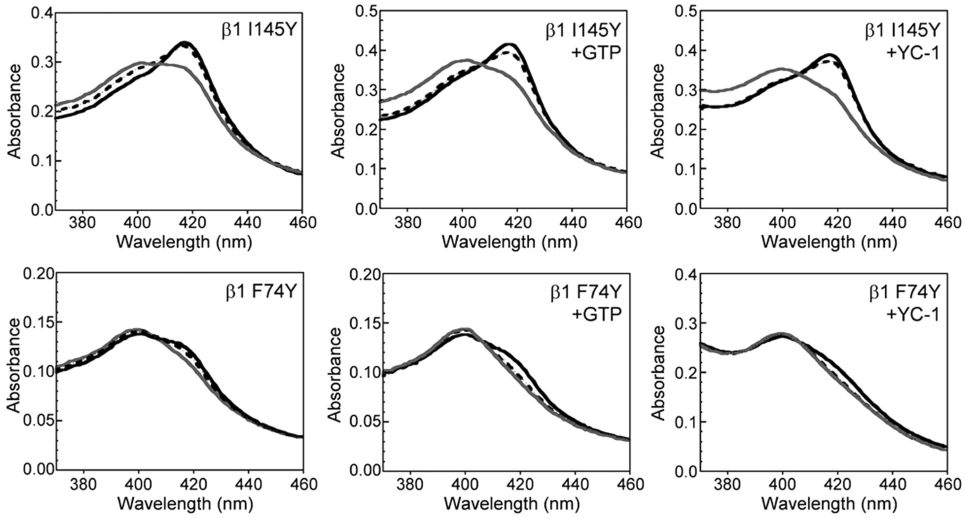

FIGURE 3. **Effect of GTP and YC-1 on the temperature-dependent equilibrium between 5- and 6-coordinate Fe^{II}-NO complexes in sGC $\alpha1\beta1$ I145Y and $\alpha1\beta1$ F74Y.** As the temperature increases from 5 to 50 °C the population of 6-coordinate sGC Fe^{II}-NO (416 nm) decreases and the population on 5-coordinate sGC Fe^{II}-NO increases (399 nm). Spectra are shown for 5 (*black solid line*), 30 (*black dashed line*), and 50 °C (*gray solid line*) for $\alpha1\beta1$ I145Y and for 5 (*black solid line*), 20 (*black dashed line*), and 30 °C (*gray solid line*) for $\alpha1\beta1$ F74Y. GTP and YC-1 lead to a greater population of the 5-coordinate Fe^{II}-NO complex.

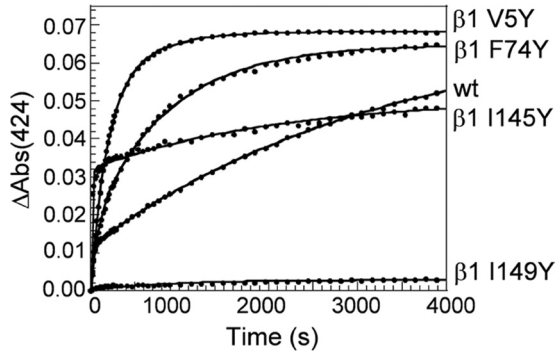

FIGURE 4. **Time courses for observed NO dissociation from sGC $\beta1$ distal pocket mutants in the presence of a CO/dithionite trap at 25 °C.** Data were extracted from difference spectra and plotted with a double (*solid line*) exponential fit. Wild-type $\alpha1\beta1$, $\alpha1\beta1$ V5Y, $\alpha1\beta1$ F74Y, $\alpha1\beta1$ I145Y, and $\alpha1\beta1$ I149Y were at 1 μM. The time courses shown are the average of duplicate dissociation experiments repeated two to four times for each construct. The low ΔAbs for the $\alpha1\beta1$ I149Y mutant is due to a very slow NO dissociation rate.

TABLE 2

Observed rate constants and fractional amplitudes for NO dissociation from $\alpha1\beta1$ sGC mutants at 25 °C

Values are averages of two to four dissociation experiments done with 1 μM protein. NO dissociation from $\beta1$ I149Y was too slow to measure.

Mutation	k_1	k_2	ΔA_1:ΔA_2
	s^{-1}	s^{-1}	%
wt	0.02696 ± 0.00698	0.00026 ± 0.000004	16:84 (±0.6)
$\beta1$ V5Y	0.00571 ± 0.00055	0.00194 ± 0.00050	70:30 (±11)
$\beta1$ F74Y	0.01120 ± 0.00318	0.00113 ± 0.00025	27:73 (±5)
$\beta1$ I145Y	0.07361 ± 0.01824	0.00044 ± 0.000003	63:37 (±3)

dependence of the Fe^{II}-NO complexes in the presence and absence of the small molecules. If GTP and YC-1 weaken the Fe-His bond, we would expect an increase in the population of 5-coordinate Fe^{II}-NO after addition of the compounds. Fig. 3 shows that 1 mM GTP and 150 μM YC-1 led to an increase in the 5-coordinate Fe^{II}-NO complex that is characterized by a Soret absorbance maximum at 399 nm in both $\alpha1\beta1$ F74Y and $\alpha1\beta1$ I145Y at all temperatures examined (5–50 °C). This result is in agreement with observations based on resonance Raman spectroscopy (33, 34).

The precise location of the allosteric substrate and YC-1 binding site remains to be determined, although there is evidence that YC-1 binds to the N terminus of the $\alpha1$ subunit (35). It has been suggested that the sGC allosteric GTP site is contained on the C terminus, within a proposed pseudosymmetric site (36–38). Although additional work is necessary to confirm these binding sites, it is clear that these compounds induce a conformational change within the heme pocket. Furthermore, the results reported here confirm that both GTP and YC-1 weaken the Fe-His bond when NO is bound to the heme.

NO Dissociation Rates—The effect of a distal pocket hydrogen bond donor on the dissociation of NO from the $\alpha1\beta1$ heme was also examined. Previously, NO dissociation from sGC was found to be complex and required two exponentials to fit the data in both the rat (29) and *Manduca sexta* (39) $\alpha1\beta1$ heterodimers. To account for this observation it was proposed that the sGC Fe^{II}-NO complex is a mixture of two different 5-coordinate species (Scheme 1).

$$\text{heme-NO}^*_{5C} \underset{k_C}{\overset{k_O}{\rightleftharpoons}} \text{heme-NO}_{5C} \underset{k_{Hd}}{\overset{k_{Hr}}{\rightleftharpoons}} \text{heme-NO}_{6C}$$
$$\xrightarrow{k_{off}} \text{heme-CO}$$

SCHEME 1

One species has a higher activity with a faster NO dissociation rate (heme-NO_{5C}), and the other species has a lower activity and slowly releases NO (heme-NO^*_{5C}). Further discussion of this model for NO dissociation from sGC can be found in a previous report (29). Additionally, analogous models have been proposed to explain multiple exponentials observed for ligand binding to hexacoordinate globins (40) and to the CO sensor CooA (41).

A CO/dithionite trap was used to measure NO dissociation from wild-type sGC and the $\beta1$ mutants V5Y, F74Y, I145Y, and I149Y at 25 °C. Plots of NO dissociation time courses for these constructs are shown in Fig. 4. The data for wild-type sGC and the $\beta1$ mutants V5Y, F74Y, and I145Y were fit to a two-exponential equation (Table 2), but the dissociation of NO from $\alpha1\beta1$ I149Y was too slow to accurately measure. This indicates that sGC $\alpha1\beta1$ I149Y forms a very stable complex with NO, and there was no significant dissociation even after 4 h at 37 °C.

The effect of a distal pocket hydrogen bond donor on k_1, the faster dissociation rate, was variable. In $\alpha1\beta1$ I145Y, both k_1 and the population of sGC with a faster NO dissociation rate increased. This construct is known to be a mixture of 5- and 6-coordinate Fe^{II}-NO complexes, and the faster dissociation

rate may arise from the population of 6-coordinate Fe^{II}-NO (32). In sGC $\alpha1\beta1$ V5Y and $\alpha1\beta1$ F74Y, k_1 decreased 5-fold and 2-fold, respectively. Additionally, the population of sGC with a faster dissociation rate increased relative to the wild-type protein. There is a difference between the observed NO dissociation rate from $\alpha1\beta1$ I145Y obtained in this report using the CO/dithionite trap (~0.07 s^{-1}) and that obtained previously from a plot of observed NO binding rates at varying NO concentrations (12–76 s^{-1}) (17). This discrepancy may be due to the different methods used to determine the rate and the limitation of measuring the rate without a stopped-flow spectrophotometer. In the previous report, the NO dissociation rate was determined by measuring NO-binding rates at varying concentrations of NO. This method does not account for the multiple exponentials observed when NO dissociates from sGC. In the current report, data scans where collected every 18 s, which is too slow to accurately measure a rate between 12 and 76 s^{-1}. Therefore the previous report likely provides a more accurate estimate of the faster NO dissociation rate, whereas results here more accurately estimate the slower dissociation rate (see below). However, it is apparent that NO dissociation is significantly affected by the inclusion of tyrosine at position 145 and that NO dissociation from $\alpha1\beta1$ I145Y is faster than that of the wild-type protein.

For all the studied constructs, the slower dissociation rate k_2, increased with the introduction of a distal pocket hydrogen bond donor. This increase in the observed rate ranged from 2-fold for $\alpha1\beta1$ I145Y to 7-fold for $\alpha1\beta1$ V5Y. Also, the relative abundance of Fe^{II}-NO with the slower dissociation rate decreased for all the mutants listed in Table 2. Although we do not have an accurate rate for NO dissociation from $\alpha1\beta1$ I149Y, we can assume that either there is an increase in the population of Fe^{II}-NO that releases NO slowly, or that there was a significant decrease in both NO dissociation rates. Regardless of the mechanism it is clear that the introduction of a tyrosine at position 149 has generated a protein that forms a remarkably stable Fe^{II}-NO complex. It is possible that NO is stabilized by a hydrogen bonding interaction with the tyrosine or alternatively, the escape of NO may be prevented by a "closed" heme pocket conformation.

Taken together, these spectroscopic studies show that the introduction of a tyrosine in the $\alpha1\beta1$ distal heme pocket significantly alters NO coordination and ligand dissociation from the heme. However, the presence of a single hydrogen bonding donor does not affect either the ability of $\alpha1\beta1$ to discriminate against O_2 binding or the stability of the Fe^{II} heme in the presence of O_2.

Activity of sGC Mutants—Importantly, some of the distal heme pocket residues that were examined in this study are conserved within the H-NOX family. Specifically, $\beta1$ Val-5 and Ile-149 are conserved residues that are proposed to be involved in maintaining the heme conformation (16). Additionally, Phe-74 and Ile-145 are residues that are involved in stabilizing O_2 binding in *Tt* H-NOX. To examine the effect of altering these residues, and potentially the sGC heme conformation, the activity of sGC after mutation of Val-5, Phe-74, Ile-145, and Ile-149 was measured (Table 3). All of the mutants exhibited a basal activity that was influenced by the presence of NO, but the

TABLE 3

Activity of various $\alpha1\beta1$ sGC mutants at 37 °C

Values for sGC determined in duplicate. The concentration of YC-1 was 150 μM.

Mutation	Ligand	Specific activity		Fold activation	
		−YC-1	+YC-1	−YC-1	+YC-1
		nmol cGMP min^{-1} mg^{-1}		*-fold*	
wt		185 ± 0	985 ± 125	1	5
	NO	13,282 ± 477	26,655 ± 5344	72	144
$\beta1$ V5Y		33 ± 12	161 ± 65	1	5
	NO	1,588 ± 588	5,162 ± 2845	48	156
$\beta1$ F74Y		433 ± 3	1,070 ± 157	1	2
	NO	5,004 ± 137	5,079 ± 1142	12	12
$\beta1$ I145Y		94 ± 11	181 ± 67	1	2
	NO	1,197 ± 68	3,216 ± 448	13	34
$\beta1$ I149Y		139 ± 0	245 ± 42	1	2
	NO	416 ± 23	1,829 ± 351	3	13

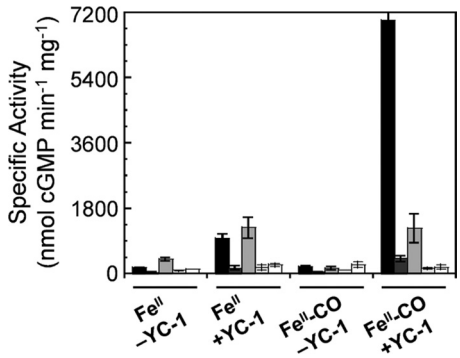

FIGURE 5. **Activity of sGC $\beta1$ distal pocket mutants in the absence and presence of CO and YC-1 at 37 °C.** The *bars*, from *left* to *right*, refer to wild-type $\alpha1\beta1$, $\alpha1\beta1$ V5Y, $\alpha1\beta1$ F74Y, $\alpha1\beta1$ I145Y, and $\alpha1\beta1$ I149Y. All constructs form 6-coordinate complexes with CO, but the Fe^{II}-CO complexes are activated to varying degrees by the presence of YC-1 (150 μM).

degree of this activation was reduced significantly in all of the mutants (supplemental Fig. S2). $\alpha1\beta1$ F74Y exhibited the highest basal activity (2-fold above wild type), while $\alpha1\beta1$ V5Y had the lowest activity in the Fe^{II}-unligated state (6-fold lower than wild type). Both $\alpha1\beta1$ F74Y and $\alpha1\beta1$ I145Y were weakly activated by NO (12- to 13-fold), but interestingly, the sGC construct that formed the most stable NO complex (sGC $\alpha1\beta1$ I149Y) exhibited the lowest degree of NO-induced activation (3-fold). This may be the result of decreasing the highly active population of the 5-coordinate Fe^{II}-NO complex, which has a fast dissociation rate.

Due to the surprisingly low activation of $\alpha1\beta1$ I149Y by NO we sought to determine if steric bulk at this position was influencing activation. Therefore, we tested the activity of sGC $\alpha1\beta1$ I149A and $\alpha1\beta1$ I149Y in Sf9 lysate after expression of the desired construct. Based on these lysate assays, $\alpha1\beta1$ I149A was activated 1.3-fold by NO, indicating the mutant exhibits reduced NO-stimulated activity. This result highlights the importance of an isoleucine at residue 149 for enzyme activation by NO.

With the exception of $\alpha1\beta1$ F74Y, the distal pocket mutants were weakly activated by CO, similar to wild-type sGC (supplemental Table S1), but YC-1 synergism was significantly reduced by the presence of a distal pocket tyrosine. YC-1 only activated the $\alpha1\beta1$ I145Y and $\alpha1\beta1$ I149Y Fe^{II}-CO complexes 1- to 2-fold, whereas the Fe^{II}-CO complexes of $\alpha1\beta1$ V5Y and $\alpha1\beta1$ F74Y were activated 8- to 10-fold (Fig. 5). This remains significantly less than the 40- to 100-fold activation observed

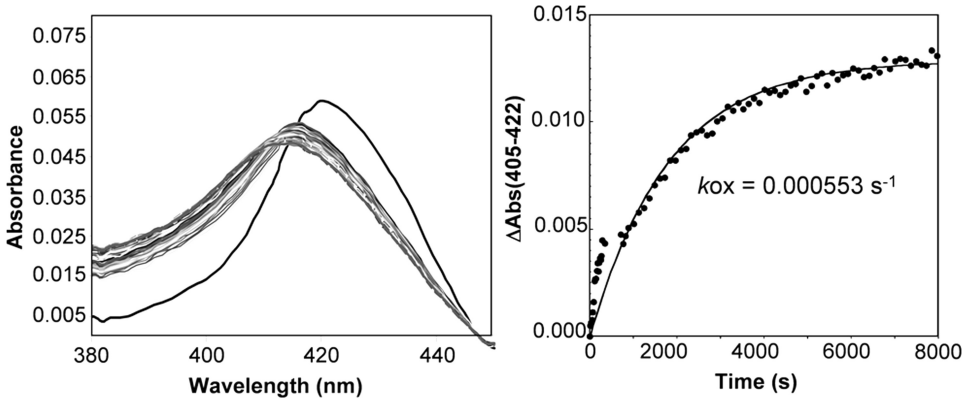

FIGURE 6. **Reaction of sGC $\alpha1\beta1$ I145Y/I149Q with O_2.** *Left panel*, reaction of sGC (500 nM) with O_2 at 10 °C. Once O_2 is added to the protein the absorbance maximum immediately shifts from 426 nm (*black trace*) to 417 nm (*dark gray trace*). Over time the 417 nm species converts to a 413 nm species (*light gray trace*). The time between each *trace* was 12 s. *Right panel*, the change in absorbance *versus* time was plotted, and data were fit to a single exponential equation.

for the wild-type protein. These results indicate that changes in the distal heme pocket can effect YC-1 binding and/or allosteric activation and confirms that the presence of the conserved residues in the heme pocket is important for sGC function. Perhaps mutation of these residues has altered the sGC heme conformation or heme pocket structure, but future work with resonance Raman spectroscopy and/or x-ray crystallography is necessary to determine if there is indeed a correlation with heme conformation and mutation of $\beta1$ Val-5 and Ile-149.

Examining the Importance of a Hydrogen Bonding Network—Although a single tyrosine residue is sufficient to stabilize O_2 binding in *Tt* H-NOX and to convert the non O_2-binding *L2* H-NOX and $\beta1(1–385)$ into O_2 binders (13), the sGC $\alpha1\beta1$ heterodimer is more complex. We found that the introduction of a single hydrogen bond donor into the sGC heme distal pocket did not lead to O_2 binding; however, proteins often utilize more than one residue to optimally position a hydrogen bond donor close to the ligand binding site (16, 28). Several truncated globins use a network involving Tyr/Gln or Tyr/Trp residues (26, 42–44), and *Tt* H-NOX uses a hydrogen bonding network primarily involving Tyr/Trp (13, 16). To investigate ligand discrimination in $\alpha1\beta1$ the sequence of the recently characterized O_2-binding guanylate cyclase Gyc-88E was examined. This protein has a tyrosine that aligns with *Tt* H-NOX Y145 in a homology model, but does not contain an asparagine or tryptophan in the predicted distal heme pocket. Instead there is a glutamine that is in close proximity to the distal pocket tyrosine residue based on a homology model (Fig. 1). To evaluate if either the *Tt* H-NOX hydrogen bonding network or the proposed Gyc-88E hydrogen bonding network can stabilize O_2 binding in sGC, the sGC double mutants $\alpha1\beta1$ L9W/I145Y and $\alpha1\beta1$ I145Y/I149Q were characterized.

The sGC mutant $\alpha1\beta1$ L9W/I145Y bound NO and CO, and was stable in the Fe^{II}-unligated heme state in the presence of O_2 (Table 1 and supplemental Fig. S3*A*). This mutant contained a greater population of 5-coordinate Fe^{II}-NO when compared to $\alpha1\beta1$ I145Y. The activity of $\alpha1\beta1$ L9W/I145Y was examined in the presence and absence of NO, CO, and YC-1 (supplemental Fig. S3*B*). The fold stimulation by NO of $\alpha1\beta1$ L9W/I145Y and wild-type $\alpha1\beta1$ was similar, despite the fact that the mutant protein contained a mixture of 5- and 6- NO coordination states. The mutant was weakly activated by CO (~2-fold), but YC-1 did not stimulate the Fe^{II}-unligated or CO-bound protein. This indicates that the addition of tryptophan at position 9 inhibits sGC stimulation by the allosteric activator.

After engineering the *Tt* H-NOX hydrogen bonding network into rat sGC, the effect of introducing the proposed Gyc-88E hydrogen bonding network was examined. Interestingly, $\alpha1\beta1$ I145Y/I149Q was isolated in the Fe^{III} heme oxidation state. The purified protein contained a substoichiometric amount of heme ($RZ = 0.09$); therefore we reconstituted $\alpha1\beta1$ I145Y/I149Q with heme ($RZ = 0.54–0.61$) and characterized the protein. Similar to our results with $\alpha1\beta1$ F74Y, $\alpha1\beta1$ I145Y/I149Q exhibited similar ligand-binding characteristics pre- and post-heme reconstitution. The mutant formed a 6-coordinate Fe^{II}-CO complex and a mixture of 5- and 6-coordinate Fe^{II}-NO complexes (Fig. 2 and Table 1). The coordination state of the Fe^{II}-NO complex was the most affected by introducing either the proposed *Tt* H-NOX or Gyc-88E hydrogen bonding networks. In sGC $\alpha1\beta1$ I145Y the NO complex is mostly 6-coordinate, and this shifts to a mostly 5-coordinate complex in both $\alpha1\beta1$ L9W/I145Y and $\alpha1\beta1$ I145Y/I149Q. The observed shift to a 5-coordinate complex in the double mutants was unexpected as *Tt* H-NOX (45) and Gyc-88E (20) form 6-coordinate complexes with NO. This indicates that distinct differences in heme pocket structure exist between the wild-type and mutagenized heme proteins.

Next, the oxidation of $\alpha1\beta1$ I145Y/I149Q was examined to investigate the possible binding of O_2 to the sGC heme. $\alpha1\beta1$ I145Y/I149Q oxidizes at a relatively fast rate (0.000553 s^{-1}) after exposure of the reduced ferrous protein to O_2. Importantly, an intermediate with an absorbance at 417 nm is observed during the oxidation reaction (Fig. 6). Fe^{II}-O_2 complexes are typically reported between 415 and 417 nm (9) strongly suggesting that the intermediate we observe is a sGC Fe^{II}-O_2 complex. To probe the oxidation state of the intermediate we added CO and/or cyanide to the 417 nm sGC species. A significant portion of the sample bound CO, as indicated by a shift in the Soret absorbance maximum from 417 to 420 nm. A small portion of the sample also bound cyanide, which is expected given the observed oxidation rate.

The activity of $\alpha1\beta1$ I145Y/I149Q in various ligation states, including the putative Fe^{II}-O_2 complex, was examined to further characterize the mutant protein (supplemental Fig. S4). $\alpha1\beta1$ I145Y/I149Q was unresponsive to the presence of CO or O_2, but was weakly activated by NO (2-fold). These results are consistent with those obtained for $\alpha1\beta1$ I149Y. The activity of Fe^{III} $\alpha1\beta1$ I145Y/I149Q was examined in the presence and absence of the ferric heme ligand cyanide. Ferric $\alpha1\beta1$ I145Y/I149Q exhibits reduced activity when compared with the activity of the ferrous protein, and enzyme activity was not affected

by CN binding. YC-1 synergistically activated the Fe^{II}-NO complex (6- to 7-fold above basal), but the allosteric activator did not stimulate the Fe^{II}-CO or putative Fe^{II}-O_2 complex. Based on this activity study, the 417 nm species does not behave like the Fe^{III} protein and more closely resembles the characteristics observed for the 6-coordinate Fe^{II}-CO complex. Although $\alpha1\beta1$ I145Y/I149Q was not stimulated by CO or O_2, its activation profile has shifted such that it is more similar to that observed for Gyc-88E, which is inhibited 3- to 2-fold by NO, CO, and O_2, than wild-type $\alpha1\beta1$.

It is apparent that the inclusion of an additional hydrogen bonding residue into the heme pocket of sGC $\alpha1\beta1$ I145Y changed the ability of the protein to interact with O_2. Significantly $\alpha1\beta1$ I145Y/I149Q is susceptible to oxidation in the presence of O_2, and we observed an intermediate in this oxidation reaction, which is likely an sGC ferrous oxy complex. This result supports the hypothesis that the absence of hydrogen bond donors in the sGC heme distal pocket is critical to the ability of the protein to discriminate against O_2 binding. Additionally, it suggests that O_2-binding sGCs like Gyc-88E stabilize O_2 binding with a hydrogen bonding network involving a tyrosine residue, as is observed in O_2-binding H-NOXs, and a glutamine residue. Several known O_2 sensors, including *Mycobacterium tuberculosis* DevS and DosT (21, 22), *Bacillus subtilis* HemAT (25), and *Desulfotalea psychrophila* HemDGC (23), also utilize a distal pocket tyrosine to selectively sense O_2. Perhaps further mutagenesis studies will elucidate the precise function of both tyrosine and glutamine for enzyme activity and ligand discrimination in this novel class of O_2-responsive cyclases.

Acknowledgments—We thank Lily Chao, Nathaniel Fernhoff, Shirley Huang, Jonathan Winger, and Michael Winter for helpful discussions and Jennifer George for technical assistance. Additionally, we thank Joey Davis and Jonathan Winger for generating homology models of H-NOX proteins.

REFERENCES

1. Münzel, T., Feil, R., Mülsch, A., Lohmann, S. M., Hofmann, F., and Walter, U. (2003) *Circulation* **108,** 2172–2183
2. Sanders, K. M., Ward, S. M., Thornbury, K. D., Dalziel, H. H., Westfall, D. P., and Carl, A. (1992) *Jpn. J. Pharmacol.* **58,** P220–P225
3. Warner, T. D., Mitchell, J. A., Sheng, H., and Murad, F. (1994) *Adv. Pharmacol.* **26,** 171–194
4. Friebe, A., Mergia, E., Dangel, O., Lange, A., and Koesling, D. (2007) *Proc. Natl. Acad. Sci. U.S.A.* **104,** 7699–7704
5. Vermeersch, P., Buys, E., Pokreisz, P., Marsboom, G., Ichinose, F., Sips, P., Pellens, M., Gillijns, H., Swinnen, M., Graveline, A., Collen, D., Dewerchin, M., Brouckaert, P., Bloch, K. D., and Janssens, S. (2007) *Circulation* **116,** 936–943
6. Boon, E. M., and Marletta, M. A. (2005) *J. Inorg. Biochem.* **99,** 892–902
7. Jain, R., and Chan, M. K. (2003) *J. Biol. Inorg. Chem.* **8,** 1–11
8. Stone, J. R., and Marletta, M. A. (1994) *Biochemistry* **33,** 5636–5640
9. Antonini, E., and Brunori, M. (1971) *Hemoglobin and Myoglobin in Their Reactions with Ligands*, North-Holland Pub. Co., Amsterdam
10. Eich, R. F., Li, T. S., Lemon, D. D., Doherty, D. H., Curry, S. R., Aitken, J. F., Mathews, A. J., Johnson, K. A., Smith, R. D., Phillips, G. N., Jr., and Olson, J. S. (1996) *Biochemistry* **35,** 6976–6983
11. Hoshino, M., Maeda, M., Konishi, R., Seki, H., and Ford, P. C. (1996) *J. Am. Chem. Soc.* **118,** 5702–5707
12. Hoshino, M., Ozawa, K., Seki, H., and Ford, P. C. (1993) *J. Am. Chem. Soc.* **115,** 9568–9575
13. Boon, E. M., Huang, S. H., and Marletta, M. A. (2005) *Nat. Chem. Biol.* **1,** 53–59
14. Deinum, G., Stone, J. R., Babcock, G. T., and Marletta, M. A. (1996) *Biochemistry* **35,** 1540–1547
15. Nioche, P., Berka, V., Vipond, J., Minton, N., Tsai, A. L., and Raman, C. S. (2004) *Science* **306,** 1550–1553
16. Pellicena, P., Karow, D. S., Boon, E. M., Marletta, M. A., and Kuriyan, J. (2004) *P. Natl. Acad. Sci. U.S.A.* **101,** 12854–12859
17. Martin, E., Berka, V., Bogatenkova, E., Murad, F., and Tsai, A. L. (2006) *J. Biol. Chem.* **281,** 27836–27845
18. Rothkegel, C., Schmidt, P. M., Stoll, F., Schröder, H., Schmidt, H. H., and Stasch, J. P. (2006) *FEBS Lett.* **580,** 4205–4213
19. Morton, D. B. (2004) *J. Biol. Chem.* **279,** 50651–50653
20. Huang, S. H., Rio, D. C., and Marletta, M. A. (2007) *Biochemistry* **46,** 15115–15122
21. Ioanoviciu, A., Meharenna, Y. T., Poulos, T. L., and Ortiz de Montellano, P. R. (2009) *Biochemistry* **48,** 5839–5848
22. Podust, L. M., Ioanoviciu, A., and Ortiz de Montellano, P. R. (2008) *Biochemistry* **47,** 12523–12531
23. Sawai, H., Yoshioka, S., Uchida, T., Hyodo, M., Hayakawa, Y., Ishimori, K., and Aono, S. (2010) *Biochim. Biophys. Acta* **1804,** 166–172
24. Wan, X., Tuckerman, J. R., Saito, J. A., Freitas, T. A., Newhouse, J. S., Denery, J. R., Galperin, M. Y., Gonzalez, G., Gilles-Gonzalez, M. A., and Alam, M. (2009) *J. Mol. Biol.* **388,** 262–270
25. Zhang, W., and Phillips, G. N., Jr. (2003) *Structure* **11,** 1097–1110
26. Martí, M. A., Capece, L., Bikiel, D. E., Falcone, B., and Estrin, D. A. (2007) *Proteins* **68,** 480–487
27. Mishra, S., and Meuwly, M. (2010) *J. Am. Chem. Soc.* **132,** 2968–2982
28. Wittenberg, J. B., Bolognesi, M., Wittenberg, B. A., and Guertin, M. (2002) *J. Biol. Chem.* **277,** 871–874
29. Winger, J. A., Derbyshire, E. R., and Marletta, M. A. (2007) *J. Biol. Chem.* **282,** 897–907
30. Woodward, J. J., Martin, N. I., and Marletta, M. A. (2007) *Nat. Methods* **4,** 43–45
31. Derbyshire, E. R., Tran, R., Mathies, R. A., and Marletta, M. A. (2005) *Biochemistry* **44,** 16257–16265
32. Boon, E. M., Davis, J. H., Tran, R., Karow, D. S., Huang, S. H., Pan, D., Miazgowicz, M. M., Mathies, R. A., and Marletta, M. A. (2006) *J. Biol. Chem.* **281,** 21892–21902
33. Li, Z. Q., Pal, B., Takenaka, S., Tsuyama, S., and Kitagawa, T. (2005) *Biochemistry* **44,** 939–946
34. Makino, R., Obayashi, E., Homma, N., Shiro, Y., and Hori, H. (2003) *J. Biol. Chem.* **278,** 11130–11137
35. Stasch, J. P., Becker, E. M., Alonso-Alija, C., Apeler, H., Dembowsky, K., Feurer, A., Gerzer, R., Minuth, T., Perzborn, E., Pleiss, U., Schröder, H., Schroeder, W., Stahl, E., Steinke, W., Straub, A., and Schramm, M. (2001) *Nature* **410,** 212–215
36. Chang, F. J., Lemme, S., Sun, Q., Sunahara, R. K., and Beuve, A. (2005) *J. Biol. Chem.* **280,** 11513–11519
37. Derbyshire, E. R., Fernhoff, N. B., Deng, S., and Marletta, M. A. (2009) *Biochemistry* **48,** 7519–7524
38. Yazawa, S., Tsuchiya, H., Hori, H., and Makino, R. (2006) *J. Biol. Chem.* **281,** 21763–21770
39. Hu, X., Murata, L. B., Weichsel, A., Brailey, J. L., Roberts, S. A., Nighorn, A., and Montfort, W. R. (2008) *J. Biol. Chem.* **283,** 20968–20977
40. Trent, J. T., 3rd, Hvitved, A. N., and Hargrove, M. S. (2001) *Biochemistry* **40,** 6155–6163
41. Puranik, M., Nielsen, S. B., Youn, H., Hvitved, A. N., Bourassa, J. L., Case, M. A., Tengroth, C., Balakrishnan, G., Thorsteinsson, M. V., Groves, J. T., McLendon, G. L., Roberts, G. P., Olson, J. S., and Spiro, T. G. (2004) *J. Biol. Chem.* **279,** 21096–21108
42. Das, T. K., Samuni, U., Lin, Y., Goldberg, D. E., Rousseau, D. L., and Friedman, J. M. (2004) *J. Biol. Chem.* **279,** 10433–10441
43. Giangiacomo, L., Ilari, A., Boffi, A., Morea, V., and Chiancone, E. (2005) *J. Biol. Chem.* **280,** 9192–9202
44. Milani, M., Pesce, A., Ouellet, Y., Dewilde, S., Friedman, J., Ascenzi, P., Guertin, M., and Bolognesi, M. (2004) *J. Biol. Chem.* **279,** 21520–21525
45. Karow, D. S., Pan, D., Tran, R., Pellicena, P., Presley, A., Mathies, R. A., and Marletta, M. A. (2004) *Biochemistry* **43,** 10203–10211